AGU PUBLICATIONS

Geophysical Research Letters

RESEARCH LETTER

10.1002/2017GL075447

# Seismic Velocity Changes in the Backarc Continental Crust After the 2011 $M_w$ 9.0 Tohoku-Oki Megathrust Earthquake

**Tae-Kyung Hong**[1], **Junhyung Lee**[1], **Donggeun Chi**[1], **and Seongjun Park**[1]

[1]Department of Earth System Sciences, Yonsei University, Seodaemun-gu Seoul, South Korea

**Key Points:**
- The regional backarc crust experiences instant seismic velocity changes after a megathrust earthquake
- The perturbed seismic velocities are recovered gradually with time
- The seismic velocity changes are strong along the great-circle directions to the event epicenter

**Supporting Information:**
- Supporting Information S1

**Correspondence to:**
T.-K. Hong,
tkhong@yonsei.ac.kr

**Citation:**
Hong, T.-K., Lee, J., Chi, D., & Park, S. (2017). Seismic velocity changes in the backarc continental crust after the 2011 $M_w$ 9.0 Tohoku-Oki megathrust earthquake. *Geophysical Research Letters*, *44*, 10,997–11,003. https://doi.org/10.1002/2017GL075447

Received 1 MAY 2017
Accepted 24 OCT 2017
Accepted article online 26 OCT 2017
Published online 14 NOV 2017



**Abstract** The 2011 $M_w$ 9.0 Tohoku-Oki megathrust earthquake accompanied coseismic and postseismic displacements around the eastern Eurasian continental plate. Noise cross correlations produced transient seismic waveforms along interstation paths in the Korean Peninsula. We measured the traveltime changes of the fundamental mode Rayleigh waves over the range of 0.03–0.08 Hz after the megathrust earthquake. The temporal seismic velocity changes in the lower crust were assessed from the traveltime changes. The traveltimes increased instantly after the megathrust earthquake and were gradually recovered over several hundreds to thousands of days. The instant shear wave velocity decreases ranged between 0.731 (±0.057)% and 4.068 (±0.173)%. The temporal medium perturbation might be caused by the transient uniaxial tensional stress due to the coseismic and postseismic displacements. The medium properties may be recovered by progressive stress field reconstruction.

## 1. Introduction

The seismic velocity is sensitive to medium perturbations, which is particularly evident in environments under low effective pressures (Brenguier et al., 2014; Shapiro, 2003; Zinszner et al., 1997). Megathrust earthquakes produce strong seismic waves and coseismic and postseismic displacements over local and regional distances. Strong seismic waves and coseismic crustal deformation incurred seismic velocity reductions ranging from 0.08 to 50% in the near surface and shallow crust over local or near-regional distances (Brenguier et al., 2014; Chaves & Schwartz, 2016; Minato et al., 2012; Nakahara, 2015; Nakata & Snieder, 2011; Taira et al., 2015; Xu & Song, 2009). Laboratory experiments reported that seismic velocities can decrease by 12–30% in granite under confining pressure (Hamiel et al., 2009; Lockner et al., 1977; Masuda et al., 1987; Stanchits et al., 2006). It was suggested that the velocity changes were caused by medium damage due to strong ground motions (Chaves & Schwartz, 2016). However, the influence of coseismic and postseismic displacements on the regional lithosphere remains veiled.

The March 11, 2011 $M_w$ 9.0 Tohoku-Oki megathrust earthquake occurred on the convergent plate boundary between the Pacific plate and the Okhotsk plate. The megathrust earthquake produced a 440 km by 180 km rupture plane with a peak coseismic slip of ~50 m (Yagi & Fukahata, 2011) (Figure 1a). The peak ground accelerations from the seismic waves reached 20–30 m/s$^2$ on the Japanese islands and ~1.5 cm/s$^2$ on the Korean Peninsula (Furumura et al., 2011; Houng et al., 2016; Tajima et al., 2013; Wu & Peng, 2011). The strong seismic waves triggered earthquakes worldwide (e.g., Houng et al., 2016; Gonzalez-Huizar et al., 2012; Miyazawa, 2011).

The peak lateral coseismic displacements reached ~4.3 m in Northern Honshu and 2–5 cm on the Korean Peninsula (Baek et al., 2012; Hong et al., 2015; Simons et al., 2011). Postseismic displacements continued following the coseismic displacements (Kim et al., 2016; Sun et al., 2014; Tobita, 2016). These cumulative postseismic displacements after the megathrust earthquake were comparable to the coseismic displacements in the Korean Peninsula. The distance-dependent discriminative displacements produced a transient uniaxial tensional stress field over the eastern Eurasian plate around the Korean Peninsula (Hong et al., 2015). We investigate the medium perturbation and its recovery in a continental intraplate region from the analysis of the seismic velocity changes.

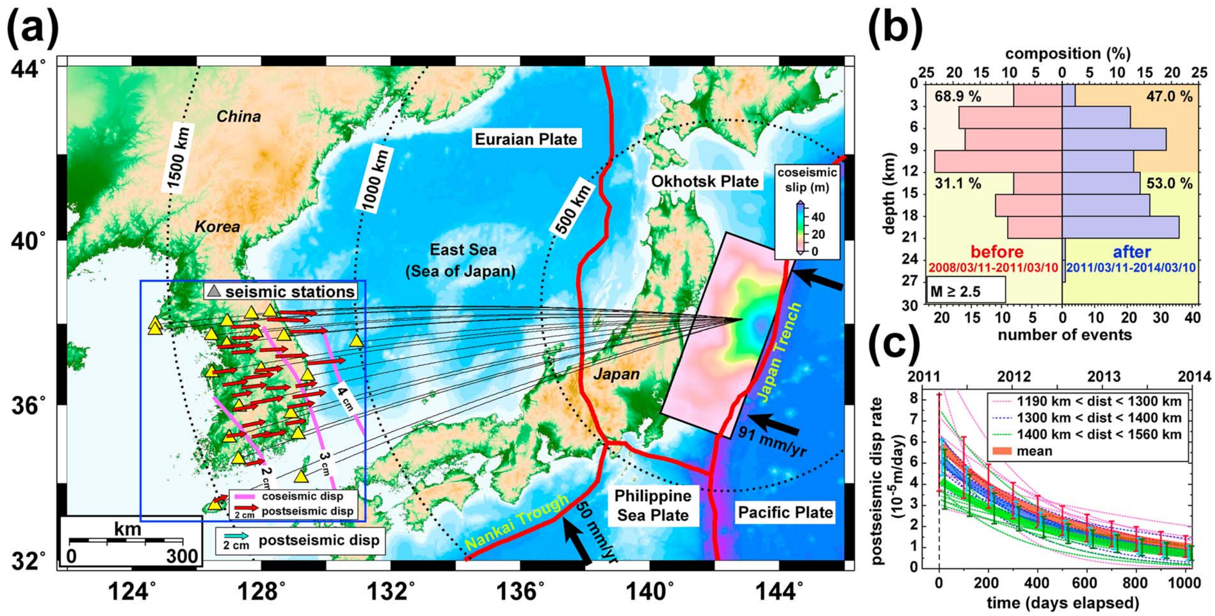


**Figure 1.** The 2011 $M_w$ 9.0 Tohoku-Oki earthquake and its effects. (a) Lateral coseismic displacements (contours with solid lines) (Hong et al., 2015) and postseismic displacements over 3 years (arrows) (Kim et al., 2016) around the Korean Peninsula. A coseismic slip model is presented (Yagi & Fukahata, 2011). The coseismic and postseismic displacements are subparallel with the great-circle directions to the epicenter. (b) Comparison of focal depth distribution before and after the megathrust earthquake. The fraction of deeper earthquakes increased for 3 years after the megathrust earthquake. (c) The postseismic displacement rates from the geodetically measured postseismic displacements (Kim et al., 2016) decrease with time, reaching less than $\sim 1 \times 10^{-5}$ m/d in ~900 days after the megathrust earthquake.

## 2. Data and Megathrust Earthquake Effects

The Korean Peninsula is located near the eastern margin of the Eurasian plate, ~1,200 to ~1,500 km away from the epicenter of the megathrust earthquake. The eastern Eurasian plate is surrounded by the Okhotsk, Pacific, and Philippine Sea plates (Figure 1a). The compressional stress induced from the convergent plate boundaries is transmitted to adjacent continental regions. The lithosphere of the Korean Peninsula consists of three Precambrian massif blocks and two intervening fold belts, which together form a stable intraplate environment. The plate disposition and intraplate environment make the Korean Peninsula a unique place for investigations of transient lithospheric deformation after a megathrust earthquake.

The Tohoku-Oki megathrust earthquake produced coseismic displacements of 2–5 cm over the Korean Peninsula (contours with solid lines in Figure 1a). The coseismic displacements constructed an epicenter-directing tension field over the peninsula (Hong et al., 2015). Postseismic displacements in the same directions followed the coseismic displacements (solid arrows in Figure 1a). The postseismic displacements at shorter distances from the epicenter were generally larger than those at longer distances. The seismicity for earthquakes with magnitudes greater than the minimum magnitude ($M_{\mathrm{min}} = 2.5$) ensuring complete records increased after the megathrust earthquake (Hong et al., 2015; Kim et al., 2016). In addition, moderate size earthquakes increased after the megathrust earthquake (Hong et al., 2015, 2017). The seismicity in the mid-crust at depths greater than 12 km increased after the megathrust earthquake, suggesting a change in the crustal stress field (Figure 1b).

The postseismic displacements decreased with time, lasting more than ~1,000 days (Kim et al., 2016) and producing negative gradients in time. The postseismic displacements at shorter distances were larger than those at longer distances (Figure 1c). These discriminative coseismic and postseismic displacements that depend on the distance to the megathrust earthquake induce a tension field in the lithosphere and the stress changes perturb the media in the crust. The increases of seismicity and focal depths in the Korean Peninsula may be associated with the decrease of yield strength by the transient tension stress (Hong et al., 2015; Watts & Burov, 2003).

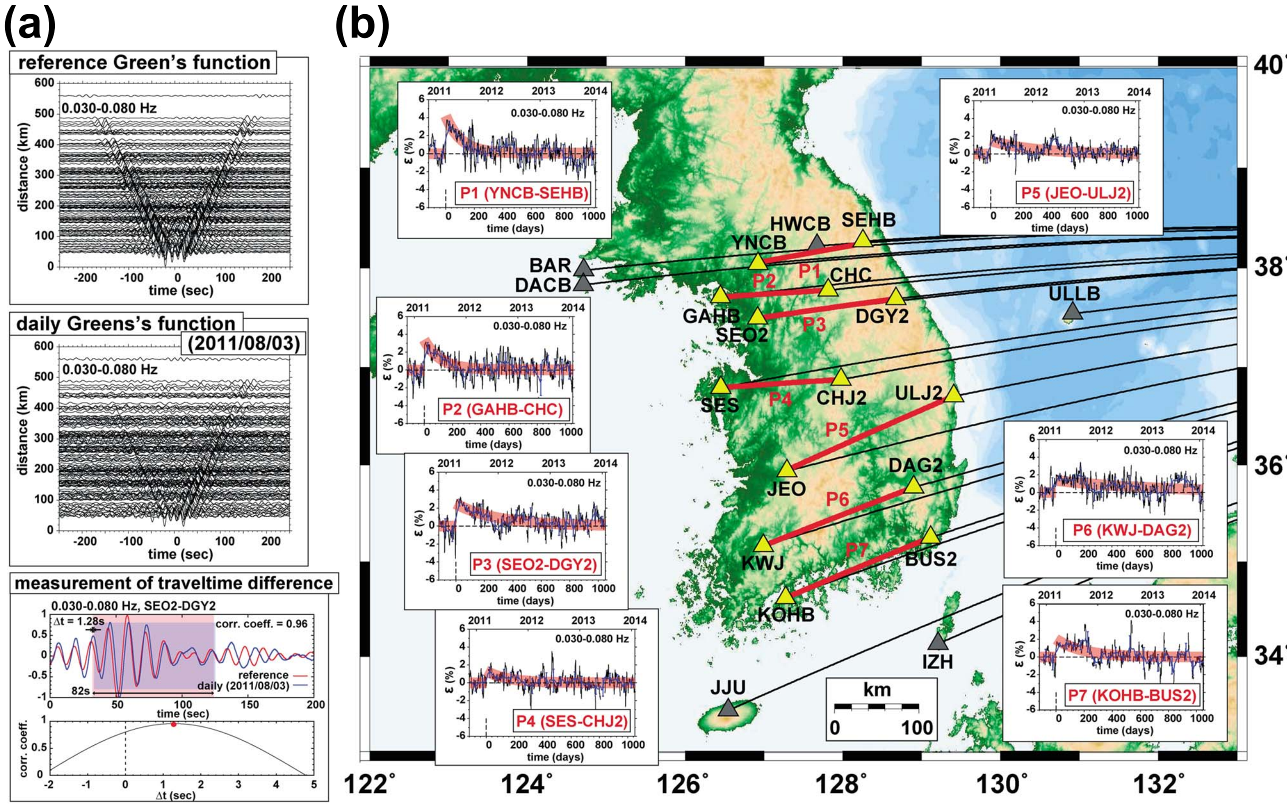

**Figure 2.** Estimation of transient seismic traveltime changes after the megathrust earthquake. (a) Reference and daily noise cross-correlation functions from ambient noise analysis, and measurement of traveltime difference using a waveform cross correlation. Noise cross-correlation functions are well retrieved. (b) Transient seismic velocity changes along some interstation paths. Instant seismic velocity decreases are observed after the megathrust earthquake (inserted figures). Parameter $\epsilon$ presents the minus of the relative velocity change. The observed seismic velocity changes are fitted by exponential functions (thick solid lines in the inserted figures). The average velocity changes over discrete time bins (blue lines) agree well with the reference exponential curves. The great-circle paths from the stations to the megathrust earthquake are presented (thin solid lines on the map).

We collected continuous seismic noise records from 20 homogeneously distributed broadband seismic stations around the Korean Peninsula from 1 September 2010 to 31 August 2014. The sampling rate of the records was 100 Hz. The interstation distances varied between 47.8 and 604.4 km. The average interstation distance was 272.4 km.

## 3. Methods

We prepared one-bit normalized seismic records of ambient noises and calculated the noise cross-correlation function for every single day for every pair of stations on the Korean Peninsula (Bensen et al., 2007; Campillo & Paul, 2003; Shapiro et al., 2005) (Figure 2). The low seismicity in the Korean Peninsula enabled us to compute stable daily noise cross-correlation functions (Figure 2). The reference noise cross-correlation function was computed from noise records for 5 months from 1 September 2010 to 28 February 2011, which represented the period before the megathrust earthquake.

We estimated the traveltime differences between the reference and daily noise cross-correlation functions using a waveform cross correlation. We selected the fundamental mode Rayleigh waveforms from the noise cross-correlation functions in lapsed time ranging between $l/v_g-10$ and $l/v_g+4.5/f_c$ s, where $l$ is the epicentral distance and $v_g$ is the group velocity of the fundamental model Rayleigh waves for the central frequency $f_c$. The fundamental mode Rayleigh waves with correlation coefficients greater than 0.8 were analyzed.

The stretch parameter $\epsilon$ was calculated from the relative time shift between the reference and daily noise cross-correlation functions, which was converted to the relative velocity change (Brenguier et al., 2008; Minato et al., 2012):

$$\epsilon = \frac{\Delta t}{t_0} \approx -\frac{v_1 - v_0}{v_0}, \tag{1}$$

where $\Delta t$ is the traveltime difference between the reference and transient traveltimes, $v_0$ is the reference seismic velocity in km/s, $v_1$ is the transient seismic velocity in km/s, and $t_0$ is the reference traveltime in seconds.

Rocks are deformed by applied stresses, accompanying seismic velocity change (Brantut et al., 2014; Schubnel et al., 2005). The recovery rates of the physical properties of elastic media are high shortly after the termination of the applied stress. The recovery rates decrease quickly with time (Brantut et al., 2014), while the seismic velocity changes with the recovery of the medium properties (Brenguier et al., 2008). The seismic velocities recover exponentially with time for release of effective stress (Brantut, 2015; Schubnel et al., 2005). Therefore, the temporal evolution of seismic velocity changes, $\epsilon$, may be represented by an exponential function:

$$\epsilon = a\exp(-by), \tag{2}$$

where the constant $a$ corresponds to the instant seismic velocity change, the constant $b$ is the seismic velocity recovery rate factor, and $y$ is the lapsed time in days. The constants $a$ and $b$ are determined for every interstation path using a nonlinear least-squares algorithm.

## 4. Noise Cross-Correlation Function

We analyzed the noise cross-correlation functions for a frequency band of 0.03 – 0.08 Hz, which was effective for a stable analysis (Xu & Song, 2009). The sensitivity kernel of the Rayleigh waves based on a one-dimensional earth model (Dziewonski & AndersonSayers, 1981) suggested that the noise cross-correlation function reflected the medium properties of the lithosphere (~9 – 84 km) (see supporting information). The wavelength for the central frequency was 67 km, which was about one fourth the average interstation distance. A detailed discussion on the analysis can be found in the supporting information (Bensen et al., 2007; Campillo & Paul, 2003; Shapiro et al., 2005; Yao et al., 2006).

We calculated the noise cross-correlation functions for the reference 5 month record sections and daily record sections (Figure 2a). The daily noise cross-correlation functions produced well-established fundamental mode Rayleigh waves. We found high correlations (correlation coefficients greater than 0.8) between the reference and daily waveform record sections in the interstation paths around the great-circle directions to the earthquake epicenter (Figure 2b; see supporting information).

It is noteworthy that the waveform correlations in the interstation paths around the great-circle directions to the earthquake epicenter temporally decreased right after the megathrust earthquake for several days (see supporting information). Also, the waveform correlations were low in the paths with deviation angles greater than about 12° from the great-circle directions to the earthquake epicenter (see supporting information).

The positive (causal) and negative (anticausal) portions of the noise cross-correlation functions were generally symmetric (see supporting information). We chose a pair of noise cross-correlation functions with large amplitudes and similarity and measured the traveltime differences of the fundamental mode Rayleigh waves.

## 5. Transient Seismic Velocity Changes

The daily fluctuations of the velocity changes before the megathrust earthquake suggested the possible error level in the velocity change estimates. The standard deviations of the daily fluctuations were generally less than 1% on most paths, which is compared to other studies (e.g., Minato et al., 2012) (Figure 2; supporting information). In addition, the velocity changes displayed the present characteristic periodic fluctuations with periods of 28.44 and 75.85 days, which could be partly associated with the solid-earth and ocean tides. The periodic fluctuations in velocity changes could reach to around 1% (supporting information). The reference noise cross-correlation functions based on 5 months records may be hardly affected by the periodic fluctuations considering the dominant frequencies.

Abrupt traveltime changes were observed after the megathrust earthquake. The traveltime differences reduced with the lapsed time after the megathrust earthquake. The seismic velocity changes were calculated from the traveltime changes from equation (1). We fitted the temporal seismic velocity changes with exponential curves. The coefficients ($a$, $b$) of the exponential curves were determined for every interstation path.

The seismic velocity changes display consistent variations that were represented well by the exponential curves (Figure 2b). We found that the instant seismic velocity decreased by 0.731 (±0.057) to 4.068 (±0.173)%

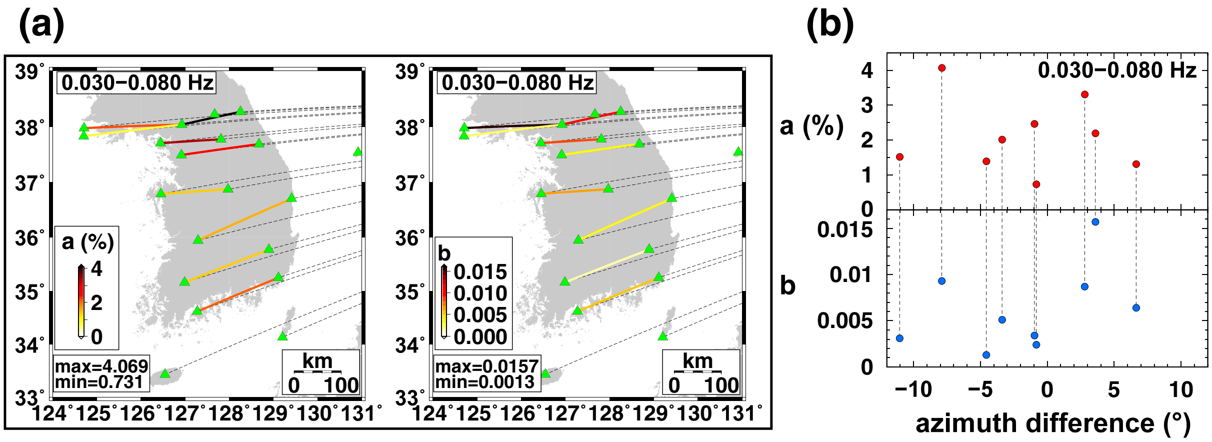


**Figure 3.** (a) Spatial distribution of instant seismic velocity changes *a* and recovery rate factors *b* and (b) variation of *a* and *b* with azimuth from the great-circle directions to the megathrust earthquake. The seismic velocity changes are observed on the paths around the great-circle directions (<12° from the great-circle directions). The recovery rates of the seismic velocities vary by path.

after the megathrust around the great-circle directions (Figure 3; see supporting information). The recovery rates (*b*) were positive, ranging between 0.0013 (±0.0001) and 0.0157 (±0.0032). The observation suggested that seismic velocities restore over time. The observed instant seismic velocity changes on some paths were much stronger than the typical levels of daily fluctuations and possible artifacts (e.g., Zhan et al., 2013). Similar velocity changes are observed in different frequencies (see supporting information).

It takes several hundreds to thousands of days to have the seismic velocity changes return to less than 0.1% according to the determined reference curves (see supporting information). The seismic velocity changes suggest that the stress field in the regional crust was perturbed by the coseismic and postseismic displacements, causing changes in medium properties. The seismicity increase in the Korean Peninsula since the megathrust earthquake supports the stress field change in the crust (Hong et al., 2015, 2017). The long-term ambient stress field perturbation in the crust may be highly affected by the static stress changes by coseismic and postseismic displacements. In contrast, the dynamic stress changes by strong seismic waves affect the transient property changes near the surface and may be less effective in the middle and deep crust due to the high-pressure confining environment (e.g., Nakata & Snieder, 2011).

## 6. Discussion and Conclusions

The 2011 *M*9.0 Tohoku-Oki megathrust earthquake accompanied large coseismic and postseismic lithospheric displacements. The stress field in the crust was perturbed by the coseismic and postseismic displacements, and the seismicity around the Korean Peninsula was increased after the megathrust earthquake (Figure 1b) (Hong et al., 2015, 2017).

We observed instant seismic velocity changes in the crust following the coseismic lithospheric displacements by the megathrust earthquake. The instant seismic velocity changes suggested a rapid response of the medium to the coseismic displacements that produced a point-directing (radio-symmetrical) tension stress field over the backarc region (Figure 4a). The seismic velocity changes generally followed an inverse of an exponential decay function with time, suggesting fast recovery of the seismic velocities shortly after the earthquake and slow recovery after some time had passed. The recovery of seismic velocities could suggest the restoration of the stress field in the crust.

The epicenter-directing lithospheric displacements were naturally subparallel with the great-circle directions to the epicenter. The point-directed extensional displacements accompanied contracting deformations in the normal directions, producing azimuth-dependent medium perturbations. The fundamental mode Rayleigh waves on the paths around the great-circle directions to the epicenter displayed high correlations in waveforms with traveltime differences before and after the megathrust (Figure 4b). The observed velocity changes were gradually recovered for several hundreds to thousands of days, which is longer than those observed in smaller events (Chaves & Schwartz, 2016; Taira et al., 2015).

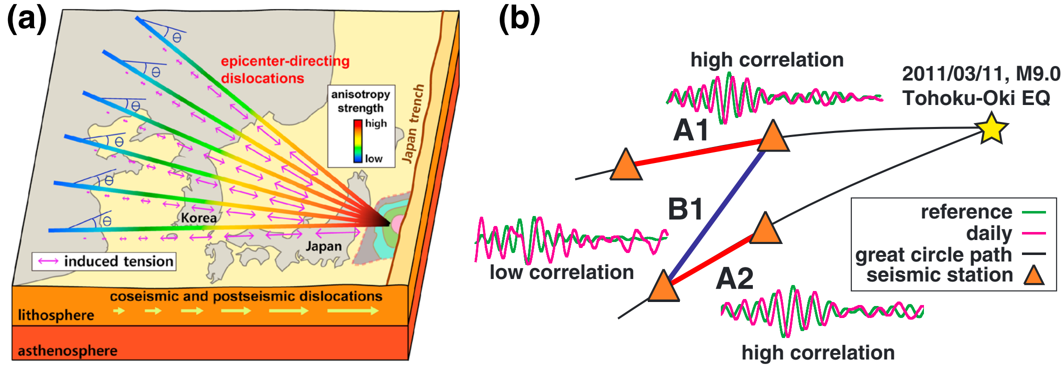


**Figure 4.** Induced tension field and traveltime changes after the megathrust earthquake. (a) Induced tension field by epicenter-directing lithospheric displacements. An epicenter-directing tension field is constructed effectively over regional distances. The induced tension stress decreases with distance. (b) Waveform correlations and traveltime difference measurement. High correlations are observed on the paths around the great-circle directions. The waveform correlations decrease on the paths off the great-circle directions due to preferential epicenter-directing medium perturbation.

In contrast, the Rayleigh waves on the paths out of the great-circle directions presented low correlations with waveforms (see supporting information). The observations suggested that the seismic waves experienced inphase traveltime changes along the great-circle directions due to the epicenter-directing lithospheric extension. However, the medium perturbation induced phase changes in the waveforms off the great-circle directions, lowering the waveform correlations. Also, we observed temporal decreases in waveform correlations even in the paths around the great-circle directions to the epicenter for several days right after the megathrust earthquake (see supporting information), which may be due to dynamic crustal deformation and viscoelastic relaxation. These features may cause difficulty in analysis of velocity changes.

The seismic velocity changes over the whole crust may be a consequence of perturbation in the static stress field and medium properties during the coseismic and postseismic lithospheric displacements. The azimuth-dependent waveform correlations suggest that epicenter-directing lithospheric displacements perturb the medium to be preferentially aligned along the induced tension axes (Hoek & Bieniawski, 1965; Lyakhovsky et al., 1997; Shimizu, 1984). It is noteworthy that the seismic velocities recover continuously during the postseismic displacements. This may be because the extensional stress (force) in the medium decreases with time due to the decreasing postseismic displacements. In addition, the static stress field can be recovered by tectonic loading during the decreasing postseismic displacements.

The medium perturbation by the megathrust earthquake appears to be particularly effective in the regional backarc region. However, the coseismic and postseismic displacements in near distances from the megathrust earthquakes cannot be simplified to be point-directing displacements as shown over regional distances. The coseismic and postseismic displacements by a megathrust earthquake with a large rupture plane may produce complicated medium deformation over near distances, which may not display obvious seismic velocity changes.

**Acknowledgments**
Most analysis results are presented in the supporting information. The continuous seismic waveform records and station information are available from Korea Meteorological Administration (necis.kma.go.kr). The authors are grateful to Andrew Newman (Editor) and two anonymous reviewers for valuable review comments that improved the presentation of this manuscript. This work was supported by the Korea Meteorological Administration Research and Development Program under grant KMIPA 2015-7040. In addition, this research was partly supported by the Basic Science Research Program through the National Research Foundation of Korea (NRF) funded by the Ministry of Education (NRF-2017R1A6A1A07015374).

## References

Baek, J., Shin, Y. H., Na, S. H., Shestakov, N. V., Park, P. H., & Cho, S. (2012). Coseismic and postseismic crustal deformations of the Korean Peninsula caused by the 2011 $M_w$ 9.0 Tohoku earthquake, Japan, from global positioning system data. *Terra Nova*, *24*, 295–300.

Bensen, G. D., Ritzwoller, M. H., Barmin, M. P., Levshin, A. L., Lin, F., Moschetti, M. P., … Yang, Y. (2007). Processing seismic ambient noise data to obtain reliable broad-band surface wave dispersion measurements. *Geophysical Journal International*, *169*, 1239–1260.

Brantut, N. (2015). Time-dependent recovery of microcrack damage and seismic wave speeds in deformed limestone. *Journal of Geophysical Research: Solid Earth*, *120*, 8088–8109. https://doi.org/10.1002/2015JB012324

Brantut, N., Heap, M. J., Baud, P., & Meredith, P. G. (2014). Rate-and strain-dependent brittle deformation of rocks. *Journal of Geophysical Research: Solid Earth*, *119*, 1818–1836. https://doi.org/10.1002/2013JB010448

Brenguier, F., Campillo, M., Hadziioannou, C., Shapiro, N. M., Nadeau, R. M., & Larose, E. (2008). Postseismic relaxation along the San Andreas fault at Parkfield from continuous seismological observations. *Science*, *321*, 1478–1481.

Brenguier, F., Campillo, M., Takeda, T., Aoki, Y., Shapiro, N. M., … Miyake, H. (2014). Mapping pressurized volcanic fluids from induced crustal seismic velocity drops. *Science*, *345*, 80–82.

Campillo, M., & Paul, A. (2003). Long-range correlations in the diffuse seismic coda. *Science*, *299*, 547–549.

Chaves, E. J., & Schwartz, S. Y. (2016). Monitoring transient changes within overpressured regions of subduction zones using ambient seismic noise. *Science Advances*, *2*(1), E1501289.

Dziewonski, A. M., & AndersonSayers, D. L. (1981). Preliminary reference Earth model. *Physics of the Earth and Planetary Interiors*, *25*, 297–356.

Furumura, T., Takemura, S., Noguchi, S., Takemoto, T., Maeda, T., Iwai, K., & Padgy, S. (2011). Strong ground motions from the 2011 off-the Pacific-Coast-of-Tohoku, Jpaan (Mw=9.0) earthquake obtained from a dense nationwide seismic network. *Landslides*, *8*, 333–338.

Gonzalez-Huizar, H., Velasco, A. A., Peng, A., & Castro, R. R. (2012). Remote triggered seismicity caused by the 2011, $M9.0$ Tohoku-Oki, Japan earthquake. *Geophysical Research Letters*, *39*, L10302. https://doi.org/10.1029/2012GL051015

Hamiel, Y., Lyakhovsky, V., Stanchits, S., Dresen, G., & Ben-Zion, Y. (2009). Brittle deformation and damage induced seismic wave anisotropy in rocks. *Geophysical Journal International*, *178*, 901–909.

Hoek, E., & Bieniawski, Z. T. (1965). Brittle fracture propagation in rock under compression. *International Journal of Fracture Mechanics*, *1*, 137–155.

Hong, T.-K., Lee, J., & Houng, S. E. (2015). Long-term evolution of intraplate seismicity in stress shadows after a megathrust. *Physics of the Earth and Planetary Interiors*, *245*, 59–70.

Hong, T.-K., Lee, J., Kim, W., Hahm, I.-K., Woo, N. C., & Park, S. (2017). The 12 September 2016 $M_L$ 5.8 mid-crustal earthquake in the Korean Peninsula and its seismic implications. *Geophysical Research Letters*, *44*, 3131–3138. https://doi.org/10.1002/2017GL072899

Houng, S. E., Lee, J., & Hong, T.-K. (2016). Dynamic seismic response of a stable intraplate region to a megathrust earthquake. *Tectonophysics*, *689*, 67–78.

Kim, D., Park, K. D., Ha, J., Sohn, D. H., & Won, J. (2016). Geodetic analysis of post-seismic crustal deformations occurring in South Korea due to the Tohoku-Oki earthquake. *KSCE Journal of Civil Engineering*, *20*, 2885–2892.

Lockner, D. A., Walsh, J. B., & Byerlee, J. D. (1977). Changes in seismic velocity and attenuation during deformation of granite. *Journal of Geophysical Research*, *82*, 5374–5378.

Lyakhovsky, V., Reches, Z. E., Weinberger, R., & Scott, T. E. (1997). Non-linear elastic behaviour of damaged rocks. *Geophysical Journal International*, *130*, 157–166.

Masuda, K., Mizutani, H., & Yamada, I. (1987). Experimental study of strain-rate dependence and pressure dependence of failure properties of granite. *Journal of Physics of the Earth*, *35*, 37–66.

Minato, S., Tsuji, T., Ohmi, S., & Matsuoka, T. (2012). Monitoring seismic velocity change caused by the 2011 Tohoku-oki earthquake using ambient noise records. *Geophysical Research Letters*, *39*, L09309. https://doi.org/10.1029/2012GL051405

Miyazawa, M. (2011). Propagation of an earthquake triggering front from the 2011 Tohoku-Oki earthquake. *Geophysical Research Letters*, *38*, L23307. https://doi.org/10.1029/2011GL049795

Nakahara, H. (2015). Auto correlation analysis of coda waves from local earthquakes for detecting temporal changes in shallow subsurface structures: The 2011 Tohoku-Oki, Japan earthquake. *Pure and Applied Geophysics*, *172*, 213–224.

Nakata, N., & Snieder, R. (2011). Near-surface weakening in Japan after the 2011 Tohoku-Oki earthquake. *Geophysical Research Letters*, *38*, L17302. https://doi.org/10.1029/2011GL048800

Schubnel, A., Fortin, J., Burlini, L., & Gueguen, Y. (2005). Damage and recovery of calcite rocks deformed in the cataclastic regime. In D. Bruhn & L. Burlini (Eds.), *High-strain zones: Structure and physical properties* (Vol. 245, pp. 203–221). London: Geological Society, Special Publications.

Shapiro, N. M., Campillo, M., Stehly, L., & Ritzwoller, M. H. (2005). High-resolution surface-wave tomography from ambient seismic noise. *Science*, *307*, 1615–1618.

Shapiro, S. A. (2003). Elastic piezosensitivity of porous and fractured rocks. *Geophysics*, *68*, 482–486.

Shimizu, N. (1984). The effect of cracks on compressional wave velocity and its anisotropy in calcareous rocks. *Geophysics*, *7*, 339–399.

Simons, M., Minson, S., Sladen, A., Ortega, F., Jiang, J., Owen, S., … Webb, F. H. (2011). The 2011 magnitude 9.0 Tohoku-Oki earthquake: Mosaicking the megathrust from seconds to centuries. *Science*, *332*, 1421–1425.

Stanchits, S., Vinciguerra, S., & Dresen, G. (2006). Ultrasonic velocities, acoustic emission characteristics and crack damage of basalt and granite. *Pure and Applied Geophysics*, *163*, 975–994.

Sun, T., Wang, K., Iinuma, T., Hino, R., He, J., Fujimoto, H., … Hu, Y. (2014). Prevalence of viscoelastic relaxation after the 2011 Tohoku-oki earthquake. *Nature*, *514*, 84–87.

Taira, T., Brenguier, F., & Kong, Q. (2015). Ambient noise-based monitoring of seismic velocity changes associated with the 2014 $M_w$ 6.0 South Napa earthquake. *Geophysical Research Letters*, *42*, 6997–7004. https://doi.org/10.1002/2015GL065308

Tajima, F., Mori, J., & Kennett, B. L. N. (2013). A review of the 2011 Tohoku-Oki earthquake (Mw 9.0): Large-scale rupture across heterogeneous plate coupling. *Tectonophysics*, *586*, 15–34.

Tobita, M. (2016). Combined logarithmic and exponential function model for fitting postseismic GNSS time series after 2011 Tohoku-Oki earthquake. *Earth, Planets and Space*, *68*, 1–12.

Watts, A. B., & Burov, E. B. (2003). Lithospheric strength and its relationship to the elastic and seismogenic layer thickness. *Earth and Planetary Science Letters*, *213*, 113–131.

Wu, C., & Peng, Z. (2011). Temporal changes of site response during the 2011 $M_W$9.0 off the Pacific coast of Tohoku earthquake. *Earth Planets and Space*, *63*, 791–795.

Xu, Z. J., & Song, X. (2009). Temporal changes of surface wave velocity associated with major Sumatra earthquakes from ambient noise correlation. *Proceedings of the National Academy of Sciences*, *106*, 14,207–14,212.

Yagi, Y., & Fukahata, Y. (2011). Rupture process of the 2011 Tohoku-oki earthquake and absolute elastic strain release. *Geophysical Research Letters*, *38*, L19307. https://doi.org/10.1029/2011GL048701

Yao, H., van Der Hilst, R. D., & Maarten, V. (2006). Surface-wave array tomography in SE Tibet from ambient seismic noise and two-station analysis—I. Phase velocity maps. *Geophysical Journal International*, *166*, 732–744.

Zhan, Z., Tsai, V. C., & Clayton, R. W. (2013). Spurious velocity changes caused by temporal variations in ambient noise frequency content. *Geophysical Journal International*, *194*, 1574–1581.

Zinszner, B., Johnson, P. A., & Rasolofosaon, P. N. J. (1997). Influence of change in physical state on elastic nonlinear response in rock: Significance of effective pressure and water saturation. *Journal of Geophysical Research*, *102*, 8105–8120.